



Combination of Radiosensitivity Gene Signature and PD-L1 Status Predicts Clinical Outcome of Patients With Locally Advanced Head and Neck Squamous Cell Carcinoma: A Study Based on The Cancer Genome Atlas Dataset

OPEN ACCESS

Dongjun Dai^{1†}, Yinglu Guo^{1†}, Yongjie Shui¹, Jinfan Li², Biao Jiang³ and Qichun Wei^{1*}

Edited by:

Yong Teng,
Emory University, United States

Reviewed by:

Vinit Shanbhag,
University of Missouri System,
United States
Amrita Mandal,
National Institutes of Health (NIH),
United States

***Correspondence:**

Qichun Wei
qichun_wei@zju.edu.cn

[†]These authors have contributed
equally to this work

Specialty section:

This article was submitted to
Molecular Diagnostics and
Therapeutics,
a section of the journal
Frontiers in Molecular Biosciences

Received: 14 September 2021

Accepted: 22 November 2021

Published: 14 December 2021

Citation:

Dai D, Guo Y, Shui Y, Li J, Jiang B and
Wei Q (2021) Combination of
Radiosensitivity Gene Signature and
PD-L1 Status Predicts Clinical
Outcome of Patients With Locally
Advanced Head and Neck Squamous
Cell Carcinoma: A Study Based on The
Cancer Genome Atlas Dataset.
Front. Mol. Biosci. 8:775562.
doi: 10.3389/fmolb.2021.775562

¹Department of Radiation Oncology, The Second Affiliated Hospital, Zhejiang University School of Medicine, Hangzhou, China,

²Department of Pathology, The Second Affiliated Hospital, Zhejiang University School of Medicine, Hangzhou, China,

³Department of Radiology, Second Affiliated Hospital, School of Medicine, Zhejiang University, Hangzhou, China

Aim: The aim of our study was to investigate the potential predictive value of the combination of radiosensitivity gene signature and PD-L1 expression for the prognosis of locally advanced head and neck squamous cell carcinoma (HNSCC).

Methods: The cohort was selected from The Cancer Genome Atlas (TCGA) and classified into the radiosensitive (RS) group and radioresistant (RR) group by a radiosensitivity-related gene signature. The cohort was also grouped as PD-L1-high or PD-L1-low based on PD-L1 mRNA expression. The least absolute shrinkage and selection operator (lasso)-based Cox model was used to select hub survival genes. An independent validation cohort was obtained from the Gene Expression Omnibus (GEO) database.

Results: We selected 288 locally advanced HNSCC patients from TCGA. The Kaplan–Meier method found that the RR and PD-L1-high group had a worse survival than others ($p = 0.033$). The differentially expressed gene (DEG) analysis identified 553 upregulated genes and 486 downregulated genes ($p < 0.05$, fold change >2) between the RR and PD-L1-high group and others. The univariate Cox analysis of each DEG and subsequent lasso-based Cox model revealed five hub survival genes (*POU4F1*, *IL34*, *HLF*, *CBS*, and *RNF165*). A further hub survival gene-based risk score model was constructed, which was validated by an external cohort. We observed that a higher risk score predicted a worse prognosis ($p = 0.0013$). The area under the receiver operating characteristic curve (AUC) plots showed that this risk score model had good prediction value (1-year AUC = 0.684, 2-year AUC = 0.702, and 3-year AUC = 0.688). Five different deconvolution methods all showed that the B cells were lower in the RR and PD-L1-high group ($p < 0.05$). Finally, connectivity mapping analysis showed that the histone deacetylase (HDAC) inhibitor trichostatin A might have the potential to reverse the phenotype of RR and PD-L1-high in locally advanced HNSCC ($p < 0.05$, false discovery rate <0.1).

Conclusion: The combination of 31-gene signature and the PD-L1 mRNA expression had a potential predictive value for the prognosis of locally advanced HNSCC who had RT. The B cells were lower in the RR and PD-L1-high group. The identified risk gene signature of locally advanced HNSCC and the potential therapeutic drug trichostatin A for the RR and PD-L1-high group are worth being further studied in a prospective homogenous cohort.

Keywords: locally advanced head and neck squamous cell carcinoma, The Cancer Genome Atlas, radiosensitivity, PD-L1, B cells, histone deacetylase inhibitor

INTRODUCTION

Head and neck cancer accounts for more than 650,000 cases and 330,000 deaths worldwide (Bray et al., 2020). Ninety percent of head and neck cancer is head and neck squamous cell carcinoma (HNSCC). HNSCC consists of a series of squamous cell cancers that developed from the mucosal surfaces of the upper aerodigestive tract, including the oral cavity, pharynx, larynx, and sinonasal tract. Nearly 60% of patients of HNSCC were diagnosed with locally advanced stage (III and IVA-B) (Vokes et al., 1993).

Radiotherapy (RT) is widely used as adjuvant therapy for locally advanced HNSCC in addition to surgery. However, the 5-year overall survival of locally advanced HNSCC remains poor, as a high local recurrent rate (50%) occurs during the disease process (Lyu et al., 2019). Recently, immunotherapy is widely considered an important strategy for the treatment of later-stage cancers. Clinical trials have demonstrated that immunotherapy improves overall survival and progression-free survival in metastatic and locally advanced cancers (Pennock and Chow, 2015). Immune checkpoint inhibitors (ICIs) pembrolizumab (MK-3475) and nivolumab (BMS-936558), which target the programmed death 1 (PD1)/programmed death ligand 1 (PD-L1) pathway, were approved for HNSCC by the US Food and Drug Administration (FDA). These two drugs were also introduced by the National Comprehensive Cancer Network as standard therapeutic methods for HNSCC (Ran and Yang, 2017). However, the response rate of ICIs in cancers is only 20%–30% (Topalian et al., 2012). Interestingly, the combination of RT therapy and immunotherapy had a synergistic effect on the treatment of cancers (Chajon et al., 2017). RT could induce the damage of cancer cells and promote tumor-specific antigens, which make the tumor visible to immune surveillance and enhance the priming and activation of cytotoxic T cells (Wang et al., 2018).

The major ICIs are the antibodies for PD-1/PD-L1 signaling pathway. The PD-1 is expressed on the surface of immune-related lymphocytes and functions as a T-cell checkpoint. It binds to PD-L1 that is often expressed on tumor cells, which subsequently inhibits the host immune response (Garber et al., 2016). The expression of PD-L1 was observed to negatively affect the prognosis of cancer patients (Thompson et al., 2004; Ghebeh et al., 2006; Xiang et al., 2018). The high PD-L1 expression was also identified to be associated with radiosensitivity (Lyu et al., 2019).

With the development of genome sequencing technology, several radiosensitivity-related gene signatures were identified (Kim et al., 2012; Ghashghaei et al., 2019; You et al., 2019),

which were useful to stratify the radioresistant (RR) and radiosensitive (RS) patients. The current study was aimed to combine the radiosensitivity-related gene signatures and the expression of PD-L1 status to classify different groups of locally advanced HNSCC and then to compare the clinical outcomes, genome profile, and immune cell infiltration in these groups. We also constructed RR- and PD-L1-high-related risk gene signatures to predict the prognosis of locally advanced HNSCC, along with the identification of possible effective drugs.

MATERIALS AND METHODS

Obtaining Locally Advanced Head and Neck Squamous Cell Carcinoma Data and the Clustering

The Cancer Genome Atlas (TCGA) HNSCC (TCGA dataset for HNSCC) RNA-seq data were acquired from the Xena database (Mary Goldman et al., 2019). Only HNSCC patients with both RNA count data and clinical information were included. The locally advanced HNSCC patients were defined as stage III, IVA, and IVB patients. The RNA count data were normalized by “TMM” method (McCarthy et al., 2012) and transformed by “voom” method from “limma” R package (Ritchie et al., 2015). The prognostic validation cohort was obtained from the Gene Expression Omnibus (GEO) database (GSE65858), which included HNSCC microarray data and clinical information.

A radiosensitivity-related 31-gene signature, which was identified based on a meta-analysis that included four different microarrays using NCI-60 cancer cell lines (Kim et al., 2012), was used to perform the clustering process. This RS signature was validated among patients with breast cancer (Jang and Kim, 2017), lower-grade glioma (Jang and Kim, 2018), and glioblastoma (Jang and Kim, 2020). The 31 genes of this signature included *ACTN1*, *ANXA2*, *ANXA5*, *ARHGDI1*, *CAPNS1*, *CBR1*, *CCND1*, *CD63*, *COR O 1A*, *CXCR4*, *DAG1*, *EMP2*, *HCLS1*, *HTRA1*, *ITGB5*, *LAPTM5*, *LRMP*, *MYB*, *PFN2*, *PIR*, *PKM*, *PTMS*, *PTPRC*, *PTPRCAP*, *PYGB*, *RAB13*, *RALB*, *SCRNI*, *SQSTM1*, *TWFI*, and *WAS*. The clustering process was performed by “kmeans” method, and two clusters were obtained. The Kaplan–Meier (KM) method was applied to the clusters, with a log-rank *p*-value calculated. The cluster with a worse overall survival was defined as RR, and the cluster with a better overall survival was defined as RS. The KM plots were also drawn for locally advanced HNSCC patients with or without RT.

Grouping of Radiosensitivity-Related Clusters With PD-L1 Expression

The optimal cutoff was explored for the PD-L1 (CD274) expression of overall locally advanced HNSCC patients when the KM methods were applied. The high and low groups of PD-L1 were then defined based on the best cutoff value. The combination of radiosensitivity-related clusters with PD-L1 expression revealed the following groups: RR and PD-L1-high group, RR and PD-L1-low group, RS and PD-L1-high group, and RS and PD-L1-low group. The KM plots of these combined groups were drawn for overall locally advanced HNSCC patients and patients with or without RT.

To further explore the detailed molecular profiles of the RR and PD-L1-high group, which had a worse overall survival than other groups, the groups were classified into the RR and PD-L1-high group and the others.

Multivariate Cox Analysis for Locally Advanced Head and Neck Squamous Cell Carcinoma

A multivariate Cox analysis for the overall, RT, and non-RT groups of locally advanced HNSCC patients was performed. The radiosensitivity, PD-L1 expression, and clinical variables that comprised age, gender, grade, stage, T and N stage, HPV and P16 status, grade, and RT experience were included in the multivariate Cox analysis.

Identification of Differentially Expressed Genes Between the Radioresistant and PD-L1-High Group and the Other Groups

The “limma” R package was used to identify the differentially expressed genes (DEGs) between the RR and PD-L1 group and the others. The DEGs were defined as the genes with a *p*-value of less than 0.05 and a fold change of over 2. The volcano plot was drawn to visualize the results of DEG identification. The DEGs were further used for the next functional analysis and survival analysis.

Functional Analysis of Differentially Expressed Genes

The functional analyses of DEGs were performed by gene ontology (GO) analysis and Kyoto Encyclopedia of Genes and Genomes (KEGG) analysis. The GO analysis consists of items that belong to biological processes (BPs), cellular components (CCs), and molecular functions (MFs). *p*-Value <0.05 and *q*-value <0.05 were set as the cutoff values. Besides, the results of logFC from the DEG analysis were used for Gene Set Enrichment Analysis (GSEA). *p*-Value <0.05 was set as the cutoff for GSEA.

Survival Analysis of Each Differentially Expressed Gene and Hub Survival Gene Selection

The univariate Cox analysis was applied for each DEG for locally advanced HNSCC patients who had RT. For each univariate Cox

analysis, the patients were divided into high and low groups based on the median expression value of the DEG. *p*-Value <0.05 was considered statistically significant. The univariate Cox analysis was also applied to the locally advanced HNSCC patients from the GEO database.

The intersect survival-related DEGs from TCGA and GEO databases were then analyzed by a least absolute shrinkage and selection operator (lasso) analysis to select hub survival genes (10-fold cross-validation was used).

Risk Score Model Construction and Validation

A risk score model was built based on hub survival genes by using the following formula: ($\beta_i \times \text{Exp}_i$) (*i* = the number of hub survival-related genes). The KM method together with the identification of the optimal cutoff value was applied for survival analysis of the risk score for locally advanced HNSCC patients who had RT. The area under the receiver operating characteristic curve (AUC) plots were drawn to estimate the reliability of the risk score. The risk score model was validated by the GEO database.

Estimation of Immune Cell Fractions

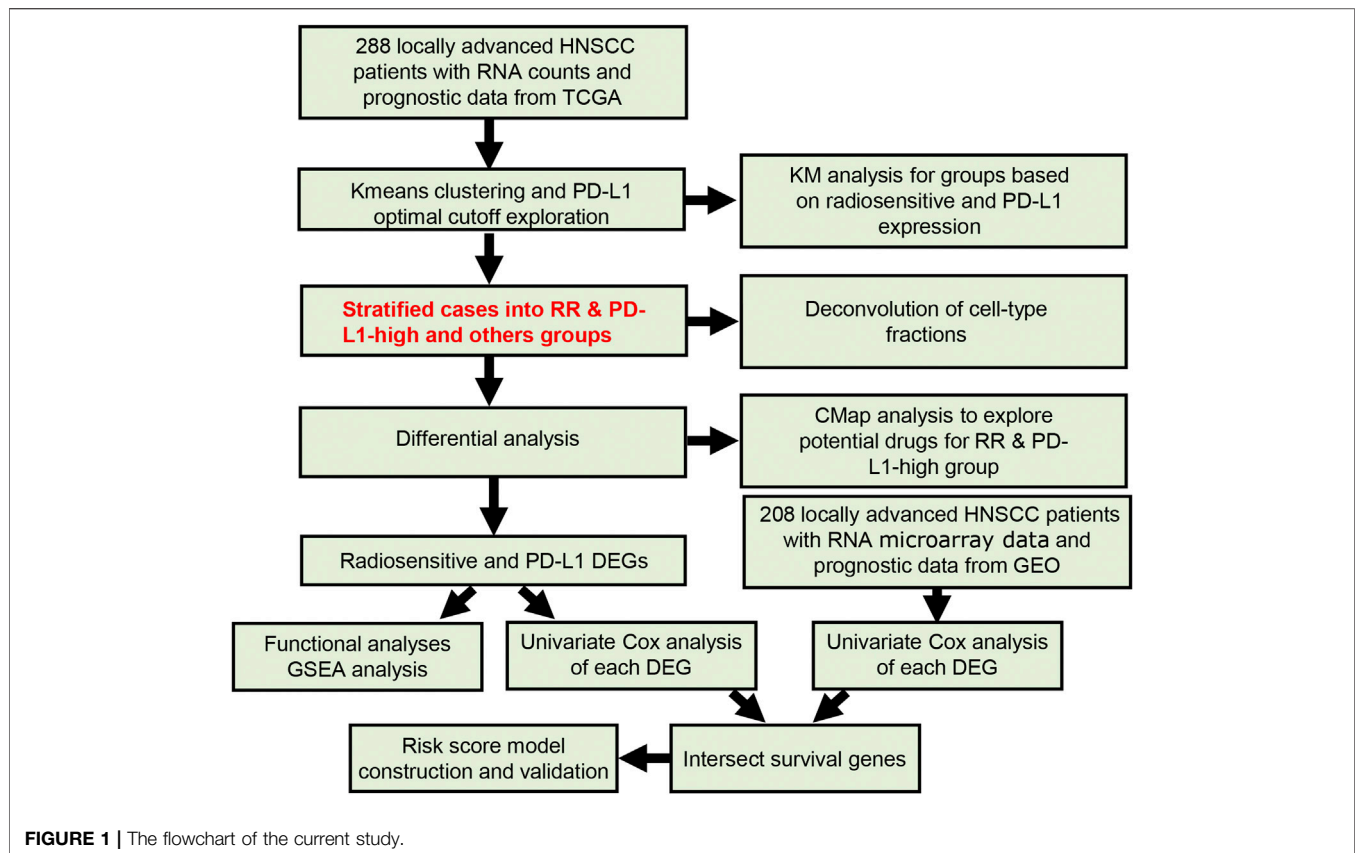
The Fragments Per Kilobase Million (FPKM) data of the locally advanced HNSCC were downloaded from Xena database and transformed to Transcripts Per Million (TPM) value. Deconvolution of cell-type fractions from RNA-seq data was calculated by xCell analysis (Aran et al., 2017), quantiseq (Finotello et al., 2019), TIMER (Li et al., 2020a), MCP-counter (Becht et al., 2016), and epic algorithms (Racle et al., 2017). The comparison was performed between the RR and PD-L1-high group and others.

Potential Therapeutic Drug Identification for Radioresistant and PD-L1-High Group

CMap analysis is a method that uses a reference drug-specific gene expression profile dataset and compares it with a disease-specific gene expression profile to identify potential drugs for a specific phenotype (Lamb, 2007; Musa et al., 2018). In the current study, the “DrInsight” R package was used to perform the CMap analysis, which aimed to find potential drugs targeted for the RR and PD-L1-high group (Chan et al., 2019). The reference profile for CMap analysis is the widely used CMap dataset, which consists of cellular signatures that catalog transcriptional responses of human cells to chemical and genetic perturbation (Subramanian et al., 2017). The function “get.cmap.ref” was used to load the CMap data matrix. The function “drug.ident” was used to connect drugs (compounds) in the CMap dataset with query data (disease phenotype, RR and PD-L1-high group). The results of the *t*-test statistic scores from the “limma” analysis were used as input data in this analysis. The identified drug should have a *p*-value <0.05 and a false discovery rate (FDR) <0.1.

Statistical Analysis

The R-4.0.2 was used for all the analyses. The chi-square analysis was applied for the clinical information of locally advanced



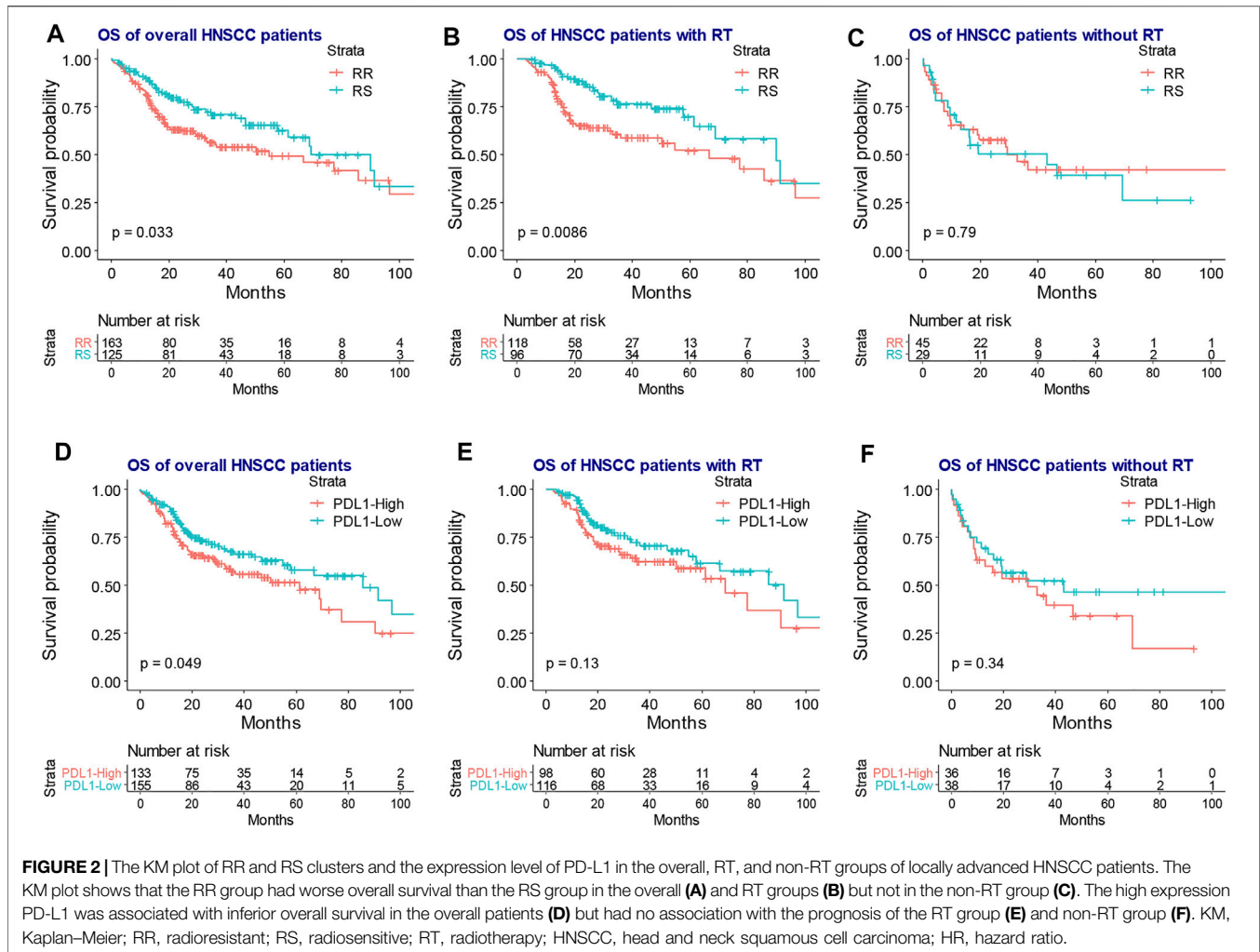
HNSCC patients with or without RT. The KM method was performed by “survminer” R package. The optimal cutoff was defined by the “surv_cutpoint” function from the “survminer” R package. The lasso method was performed by “glmnet” R package. The deconvolution of cell-type fractions was calculated by “immunedeconv” R package. The functional analyses and GSEA were performed by “clusterProfiler” R package. The AUC plot was drawn by “ROCR” R package. The Wilcoxon analysis and Kruskal–Wallis analysis were used for the comparisons between two groups and three groups, respectively.

RESULTS

Gene Signature Clustering and PD-L1 Grouping

As shown in **Figure 1**, RNA count data and clinical information of 288 locally advanced HNSCC patients were collected from TCGA database. The median age of locally advanced HNSCC patients was 61 years (interquartile range = 14). The median overall survival of locally advanced HNSCC patients was 22.65 months (interquartile range = 30.08). After the clustering analysis by 31 radiosensitivity-related genes, two clusters were identified. KM method found a significant prognostic difference between the two clusters (**Figure 2A**, $p = 0.033$). The same analysis was also applied for locally advanced HNSCC patients

with or without RT. The significant prognostic difference was observed to be only existing in the RT group (**Figure 2B**, $p = 0.0088$) but not in the non-RT group (**Figure 2C**, $p = 0.79$). Higher expression of PD-L1 was also observed to be associated with worse overall survival in the overall group (**Figure 2D**, $p = 0.049$) but not in the RT or non-RT group (**Figures 2E,F**, $p = 0.13$ and 0.34 for the RT and non-RT groups, respectively), which might be a result of the inadequate patient sample. Based on the radiosensitivity analysis and the expression level of PD-L1 of locally advanced HNSCC patients, the overall patients were stratified into four groups, as follows: RR and PD-L1-high group, RR and PD-L1-low group, RS and PD-L1-high group, and RS and PD-L1-low group. Among these four groups, the KM method observed significant prognostic differences in overall patients (**Figure 3A**, $p = 0.016$) and patients with RT (**Figure 3B**, $p = 0.011$) but not in patients without RT (**Figure 3C**, $p = 0.79$). Further focus was on the survival of the RR and PD-L1-high group, which had the worst overall survival than others. It was observed that the RR and PD-L1-high group had worse survival than others in overall patients (**Figure 3D**, $p = 0.033$) and patients with RT (**Figure 3E**, $p = 0.035$) but not in patients without RT (**Figure 3F**, $p = 0.74$). Therefore, the following analyses, including the multivariate Cox analysis, DEG analysis, immune cell fraction identification, and target drug exploration, were applied in the comparisons between the RR and PD-L1-high group and others.



Multivariate Cox Analysis for Locally Advanced Head and Neck Squamous Cell Carcinoma Patients

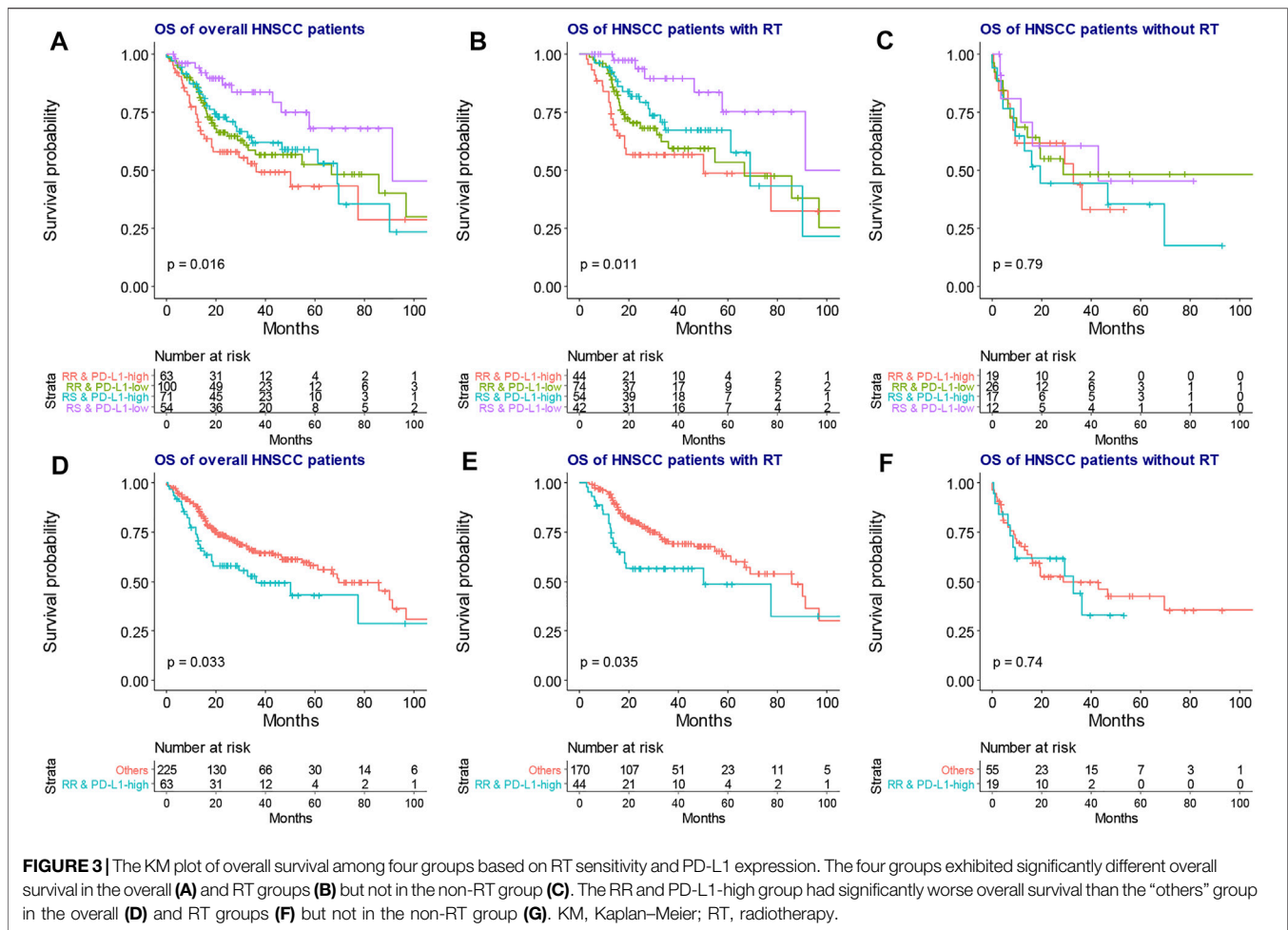
The baseline characteristics of locally advanced HNSCC patients are listed in **Table 1**. Compared with the non-RT group, the RT group had patients with younger age (RT vs. non-RT = 0.551 vs. 0.311, $p < 0.001$), more stage IVa and IVb (RT vs. non-RT = 0.757 vs. 0.595, $p = 0.012$), and more HPV negative status (RT vs. non-RT = 0.159 vs. 0.054, $p = 0.024$). No other significant results were found between the RT and non-RT groups ($p > 0.05$).

Multivariate Cox analyses were performed for overall locally advanced HNSCC and patients with or without RT. As shown in **Table 2**, for the overall group, male patients were found to have better survival than female patients (hazard ratio (HR) = 0.59, 95%CI = 0.38–0.92, $p = 0.02$), patients with positive margin status had worse overall survival than patients with negative margin status (HR = 2.73, 95%CI = 1.57–4.75, $p < 0.001$), the RS group had better survival than the RR group (HR = 0.51, 95%CI = 0.32–0.80, $p = 0.003$), the PD-L1-low group had better survival than the PD-L1-high group (HR = 0.57,

95%CI = 0.38–0.87, $p = 0.008$), and the RT group had better survival than the non-RT group (HR = 0.48, 95%CI = 0.31–0.73, $p < 0.001$). For the RT group, consistent with the overall group, patients with positive margin status had worse overall survival than patients with negative margin status (HR = 3.57, 95%CI = 1.81–7.01, $p < 0.001$), the RS group had better survival than the RR group (HR = 0.38, 95%CI = 0.21–0.67, $p = 0.001$), the PD-L1-low group had better survival than the PD-L1-high group (HR = 0.44, 95%CI = 0.26–0.74, $p = 0.002$). On the other hand, for the non-RT group, there was no association between the margin status or radiosensitivity or PD-L1 level and the prognosis of patients ($p > 0.05$).

Differentially Expressed Gene Identification Between Radioresistant and PD-L1-High and Other Groups

As the volcano plot shows (**Figure 4A**), the DEG analysis identified 553 upregulated DEGs and 486 downregulated DEGs (**Supplementary Table S1**, p -adjust value < 0.05). The functional analyses found that the immunoglobulin, immune



response, and metabolism-related items were strongly associated with the DEGs by GO and KEGG analyses (Figure 4B, Supplementary Table S2–5). The GSEA also observed that the immunoglobulin and cell metabolism-related items were upregulated in the RR and PD-L1-high group, while the epithelium development and differentiation-related items and the JAK-STAT signaling pathway were downregulated in the RR and PD-L1-high group (Figures 4C,D, Supplementary Table S6).

Survival Analysis of Each Differentially Expressed Gene and Hub Survival Gene Selection

The DEGs were further analyzed by univariate Cox model to acquire the survival-related DEGs for locally advanced HNSCC patients who had RT. A total of 213 survival-related DEGs were identified (Supplementary Table S7, $p < 0.05$). Among these survival-related DEGs, there were 123 survival favorable genes and 90 survival unfavorable genes. A univariate Cox model was also performed among locally advanced HNSCC from the GEO database (Supplementary Table S7, $p < 0.05$). The intersect 15 survival-related genes

between TCGA and GEO databases were selected for further analysis.

Next, a lasso-based Cox model was performed for locally advanced HNSCC patients who had RT by including the intersect survival-related genes. *POU4F1*, *IL34*, *HLF*, *CBS*, and *RNF165* were identified as hub survival genes, as they had nonzero coefficient values by the lasso analysis (Supplementary Table S8). The KM plots and forest plots of these hub survival genes are shown in Figure 5.

Risk Score Model Construction and Validation

A risk score model based on hub survival genes was further constructed. The KM method together with the exploration of optimal cutoff found that a higher risk score was significantly associated with the inferior overall survival of locally advanced HNSCC patients who had RT (Figure 6A, $p = 0.0013$). The AUC plots showed that the risk score had a good prediction value (1-year AUC = 0.684, 2-year AUC = 0.702, and 3-year AUC = 0.688, Figure 6B). A validation of this risk score model was performed for locally advanced HNSCC patients from the GEO database (log-rank p -value

TABLE 1 | The clinical characteristics of overall, RT, and non-RT groups of patients with locally advanced HNSCC.

Characteristics	Overall HNSCC	RT group	Non-RT group	p-Value
	No. of patients (%)	No. of patients (%)	No. of patients (%)	
Age				<0.001
High	147 (0.51)	96 (0.449)	51 (0.689)	
Low	141 (0.49)	118 (0.551)	23 (0.311)	
Gender				0.242
Female	62 (0.215)	42 (0.196)	20 (0.27)	
Male	226 (0.785)	172 (0.804)	54 (0.73)	
Stage				0.012
Stage III	82 (0.285)	52 (0.243)	30 (0.405)	
Stage IV	206 (0.715)	162 (0.757)	44 (0.595)	
T stage				0.305
T1–2	50 (0.174)	35 (0.164)	15 (0.203)	
T3	103 (0.358)	73 (0.341)	30 (0.405)	
T4	135 (0.469)	106 (0.495)	29 (0.392)	
N stage				0.203
N0	98 (0.34)	69 (0.322)	29 (0.392)	
N1	66 (0.229)	46 (0.215)	20 (0.27)	
N2–3	119 (0.413)	94 (0.439)	25 (0.338)	
NA	5 (0.017)	5 (0.023)	-	
HPV status				0.024
Negative	38 (0.132)	34 (0.159)	4 (0.054)	
Positive	11 (0.038)	10 (0.047)	1 (0.014)	
NA	239 (0.83)	170 (0.794)	69 (0.932)	
P16 status				0.056
NA	223 (0.774)	159 (0.743)	64 (0.865)	
Negative	48 (0.167)	39 (0.182)	9 (0.122)	
Positive	17 (0.059)	16 (0.075)	1 (0.014)	
Grade				0.051
G1–2	207 (0.719)	147 (0.687)	60 (0.811)	
G3–4	71 (0.247)	57 (0.266)	14 (0.189)	
NA	10 (0.035)	10 (0.047)		
Margin status				0.0634
NA	34 (0.118)	27 (0.126)	7 (0.095)	
Close	25 (0.087)	14 (0.065)	11 (0.149)	
Negative	199 (0.691)	147 (0.687)	52 (0.703)	
Positive	30 (0.104)	26 (0.121)	4 (0.054)	
Radiosensitivity and PD-L1 groups				0.451
Others	225 (0.781)	170 (0.794)	55 (0.743)	
RR and PD-L1-high	63 (0.219)	44 (0.206)	19 (0.257)	
Radiotherapy				-
No	74 (0.257)	-	-	
Yes	214 (0.743)	-	-	
PD-L1 level				0.773
High	134 (0.465)	98 (0.458)	36 (0.486)	
Low	154 (0.535)	116 (0.542)	38 (0.514)	

Note. The significant results of chi-square analysis are bolded. The p-value describes the difference between RT and non-RT groups. RT, radiotherapy; HNSCC, head and neck squamous cell carcinoma; RR, radioresistant.

= 0.0018, 1-year AUC = 0.687, 2-year AUC = 0.646, and 3-year AUC = 0.671, **Figures 6C,D**).

Estimation of Immune Cell Fractions Between Radioresistant and PD-L1-High and Other Groups

As shown in **Figure 7**, xCell analysis, quantiseq, TIMER, MCP-counter, and epic all identified that the RR and PD-L1-high group had lower B-cell infiltration than the others ($p < 0.05$, **Figure 7** and **Supplementary Table S9–3**). The detailed immune cell

fractions level calculated by five algorithms are listed in **Supplementary Table S9–13**.

Identification of Trichostatin A as the Potential Drug for Radioresistant and PD-L1-High Group

As shown in **Table 3**, the CMap analysis found that trichostatin A was the potential drug that might reverse the phenotype of the RR and PD-L1-high group ($p < 0.05$ and FDR < 0.1).

TABLE 2 | The multivariate analysis of overall, RT, and non-RT groups of patients with locally advanced HNSCC.

Characteristics	Overall HNSCC		RT group		Non-RT group	
	HR (95%CI)	p-Value	HR (95%CI)	p-Value	HR (95%CI)	p-Value
Age						
High	Reference					
Low	0.91 (0.60–1.38)	0.667	1.02 (0.61–1.71)	0.928	0.50 (0.21–1.21)	0.125
Gender						
Female	Reference					
Male	0.59 (0.38–0.92)	0.020	0.63 (0.35–1.14)	0.127	0.45 (0.21–0.96)	0.039
Stage						
Stage III	Reference					
Stage IV	1.38 (0.60–3.19)	0.447	1.53 (0.51–4.57)	0.450	4.66 (0.77–28.22)	0.094
T stage						
T1–2	Reference					
T3	1.25 (0.63–2.47)	0.527	1.17 (0.46–2.96)	0.746	2.92 (0.81–10.54)	0.102
T4	0.92 (0.42–2.04)	0.840	0.68 (0.23–1.97)	0.479	1.24 (0.26–5.93)	0.791
N stage						
N0	Reference					
N1	1.05 (0.61–1.79)	0.863	0.62 (0.31–1.25)	0.181	4.34 (1.43–13.12)	0.009
N2–3	1.19 (0.62–2.28)	0.606	1.07 (0.47–2.44)	0.874	0.86 (0.24–3.05)	0.816
NA	0.00 (0.00–Inf)	0.995	0.00 (0.00–Inf)	0.996	NA	NA
HPV status						
Negative	Reference					
Positive	0.21 (0.02–2.30)	0.202	0.34 (0.03–4.54)	0.414	0.00 (0.00–Inf)	0.997
NA	0.80 (0.30–2.09)	0.642	0.75 (0.24–2.37)	0.626	0.38 (0.03–4.14)	0.425
P16 status						
Negative	Reference					
Positive	0.89 (0.16–5.09)	0.897	0.36 (0.03–4.07)	0.405	8.28 (0.23–302.13)	0.250
NA	1.08 (0.45–2.57)	0.867	1.17 (0.38–3.53)	0.788	1.10 (0.19–6.33)	0.918
Grade						
G1–2	Reference					
G3–4	0.95 (0.60–1.52)	0.845	1.01 (0.59–1.75)	0.960	1.11 (0.37–3.32)	0.857
NA	0.92 (0.11–7.57)	0.940	1.12 (0.13–9.75)	0.922	NA	NA
Margin status						
Negative	Reference					
Close	0.47 (0.18–1.22)	0.119	0.20 (0.03–1.47)	0.113	0.65 (0.19–2.18)	0.481
Positive	2.73 (1.57–4.75)	<0.001	3.57 (1.81–7.01)	<0.001	1.00 (0.25–4.04)	0.997
NA	0.80 (0.37–1.74)	0.571	0.91 (0.34–2.41)	0.846	0.55 (0.09–3.21)	0.504
Radiosensitivity						
RR	Reference					
RS	0.51 (0.32–0.80)	0.003	0.38 (0.21–0.67)	0.001	0.60 (0.26–1.41)	0.244
PD-L1 level						
High	Reference					
Low	0.57 (0.38–0.87)	0.008	0.44 (0.26–0.74)	0.002	0.68 (0.31–1.49)	0.335
Radiotherapy						
No	Reference					
Yes	0.48 (0.31–0.73)	<0.001	NA	NA	NA	NA

Note. The significant results of multivariate Cox analysis are bolded.

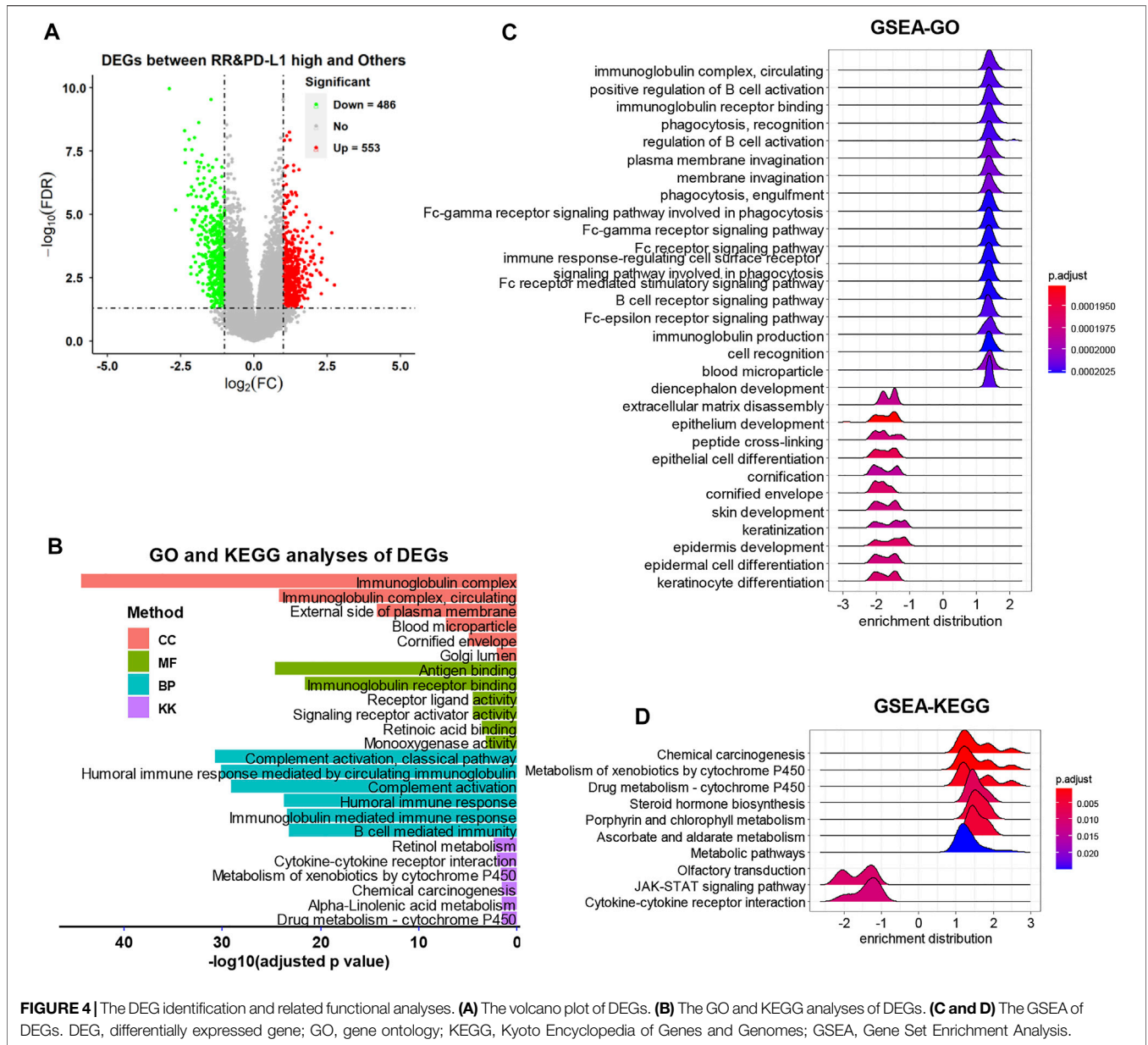
RT, radiotherapy; HNSCC, head and neck squamous cell carcinoma; HR, hazard ratio; RR, radioresistant; RS, radiosensitive; NA, not available.

DISCUSSION

Higher PD-L1 gene expression was found to be associated with an inferior prognosis of head and neck cancer (Lin et al., 2015; García-Pedrero et al., 2017; Müller et al., 2017). The current study first combined the 31-radiosensitivity gene signature and the PD-L1 gene expression to predict the prognosis of locally advanced HNSCC. We found the RR and PD-L1-high group had significantly worse survival than others when HNSCC patients were treated with RT. The RR and PD-L1-high group might potentially benefit from a combination of RT and immunotherapy, which requires further clinical trials.

RS tumors are more frequently present in patients with a phenotype of immune activation (Strom et al., 2017). The

estimation of immune cell fractions in HNSCC found that the B cells were significantly higher in other groups than in the RR and PD-L1-high group. It was identified by five different algorithms. A systematic review showed that B cells play a beneficial role in the majority of cancer types (Wouters and Nelson, 2018). A B cell-associated signature was found to distinguish HPV-positive from HPV-negative HNSCC (Wood et al., 2016). High abundance of B cells in the tumor microenvironment and high density of direct B cell/CD8+ T-cell interactions were found to be associated with an excellent prognosis of oropharyngeal squamous cell carcinoma patients (Hladíková et al., 2019). Moreover, B cells could improve the overall survival in HPV-associated HNSCC and be activated

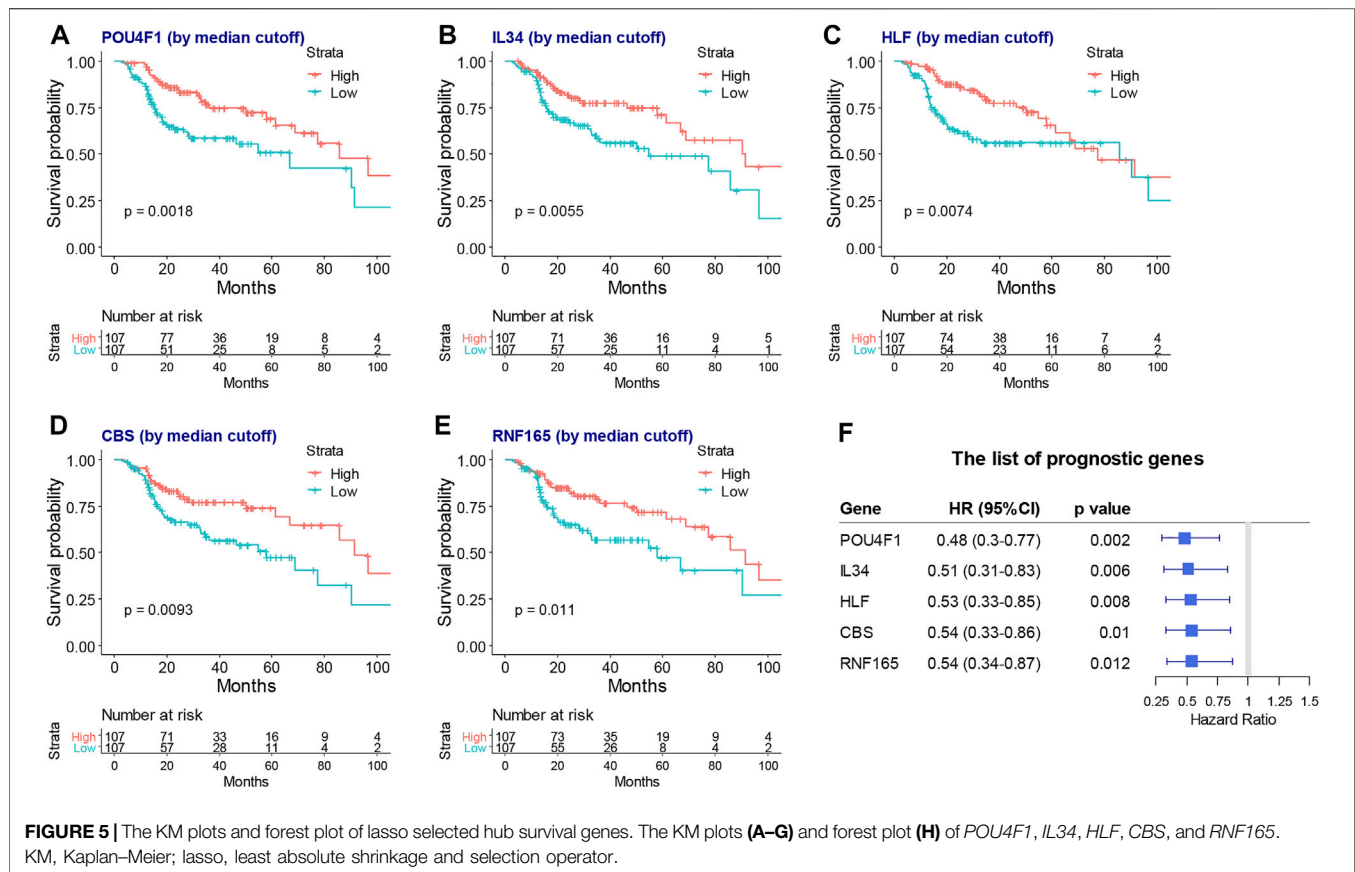


by radiation and PD-1 blockade (Kim et al., 2020). We found the B cells were significantly lower in the RR and PD-L1-high group, which proved the new insight into the association between B cells and HNSCC prognosis.

The function analysis revealed several items that were associated with the RR and PD-L1-high group. Among them, many metabolism-related pathways were found to be upregulated in the RR and PD-L1-high group, such as metabolism of xenobiotics by cytochrome P450, drug metabolism–cytochrome P450, ascorbate and aldarate metabolism, and porphyrin and chlorophyll metabolism. Metabolic reprogramming is considered one of the hallmarks of cancer (Hanahan and Weinberg, 2011). Previous studies identified that the changes in glucose, mitochondrial, lactic acid, and other metabolic processes influenced cellular radioresistance (Tang et al., 2018). Our study again proved the

importance between metabolism and radioresistance. However, this needs to be further explored by detailed molecular experiments.

By using the lasso analysis, we built a risk score model for TCGA patients with locally advanced HNSCC who had RT. *POU4F1*, *IL34*, *HLE*, *CBS*, and *RNF165* were identified as hub survival genes. We found that higher expression of these five genes was associated with favorable overall survival. The HPV-associated HNSCC has a better survival rate due to a higher sensitivity to chemotherapy and RT as compared with HPV-unrelated HNSCC (Liu et al., 2018a). *POU4F1* as a cellular transactivator was shown to be expressed at elevated levels in squamous cell carcinoma of the cervix and to activate the expression of HPV E6 mRNA (Ndisang et al., 2009). It was also found that the *POU4F1* suppressed tumor metastasis via c-MET/STAT3 inhibition and EMT suppression in thyroid cancer (Jung et al., 2020). Interleukins could directly or indirectly stimulate



cancer-cell proliferation, survival, and diffusion, which are secreted from cancer cells or immune cells among the tumor immune microenvironment. IL-34 plays a controversial role in cancer. In some cancers, IL-34 inhibits cancer cell proliferation and motility, as well as monocyte-like cell differentiation, such as lung cancer (Wang et al., 2021), while it also plays a tumor-promoting role by acting directly on transformed cells to increase their proliferation in a series of cancers (Franzè et al., 2020). Downregulation of the circadian rhythm regulator HLF promotes multiple-organ distant metastases in non-small cell lung cancer through PPAR/NF- κ B signaling (Chen et al., 2020). Lower HLF expression was correlated with more advanced renal cell carcinoma (RCC) (Huang et al., 2020) and HNSCC (Liu et al., 2021). Positive CBS is closely associated with a decreased overall survival in patients with gallbladder squamous cell carcinomas or gallbladder adenocarcinomas (Li et al., 2020b). Reduced CBS expression was observed to be significantly correlated with higher tumor stage, higher grade, and shorter overall survival of hepatocellular carcinoma (Kim et al., 2009). No evidence was found between RNF165 and cancers. Few studies were found on these key survival genes and HNSCC. Our study proved new indications between these genes and radiosensitivity, immune response, and the prognosis of HNSCC.

RT was identified to be associated with the activation of the immune system. The radiation induces tumor cell death and the release of cancer neoantigens and damage-associated molecular patterns (DAMPs). The DAMPs would recruit and facilitate the maturation of the antigen-presenting cells (APCs) in their uptake

in the irradiated cancer cells. The APCs would then present the cancer neoantigens to T cells. The T cells would be activated and migrate to the tumor microenvironment including primary tumors and non-irradiated tumor metastases, exerting the antitumor effect, which is defined as the abscopal effect (Liu et al., 2018b). However, the binding between the PD-L1 of the tumor cell and the PD-1 of the T cell would inhibit immune responses. The development of an ICI that targets the PD-1 and PD-L1 was shown to enhance the antitumor immunity of RT (Liu et al., 2018b). The combination of RT and anti-PD-1/PD-L1 antibody is a promising strategy supported by a number of preclinical and clinical evidences (Sato et al., 2020).

Utilizing CMap analysis, we found that trichostatin A, which is a pan-histone deacetylase (pan-HDAC) inhibitor of class I and II HDACs, could reverse the phenotype of the RR and PD-L1-high group. Through the deacetylation of histone proteins, HDACs play a critical role in the regulation of transcription (Kulka et al., 2020). The upregulation of specific HDACs has been found in a series of cancers that included HNSCC (Kumar et al., 2015; Li and Seto, 2016). There was a synergistic antitumor activity of HDAC inhibitor SAHA and EGFR inhibitor gefitinib in HNSCC (Citro et al., 2019). The combined use of HDAC inhibitor and RT led to a synergistic effect, which reduced toxicity and diminished intrinsic and acquired resistance in cancer patients (Shirbhate et al., 2020). A study found that trichostatin A increased radiosensitivity of tongue squamous cell carcinoma via miR-375 (Jia et al., 2017). Besides, HDAC inhibitors were found to be associated with immunotherapy.

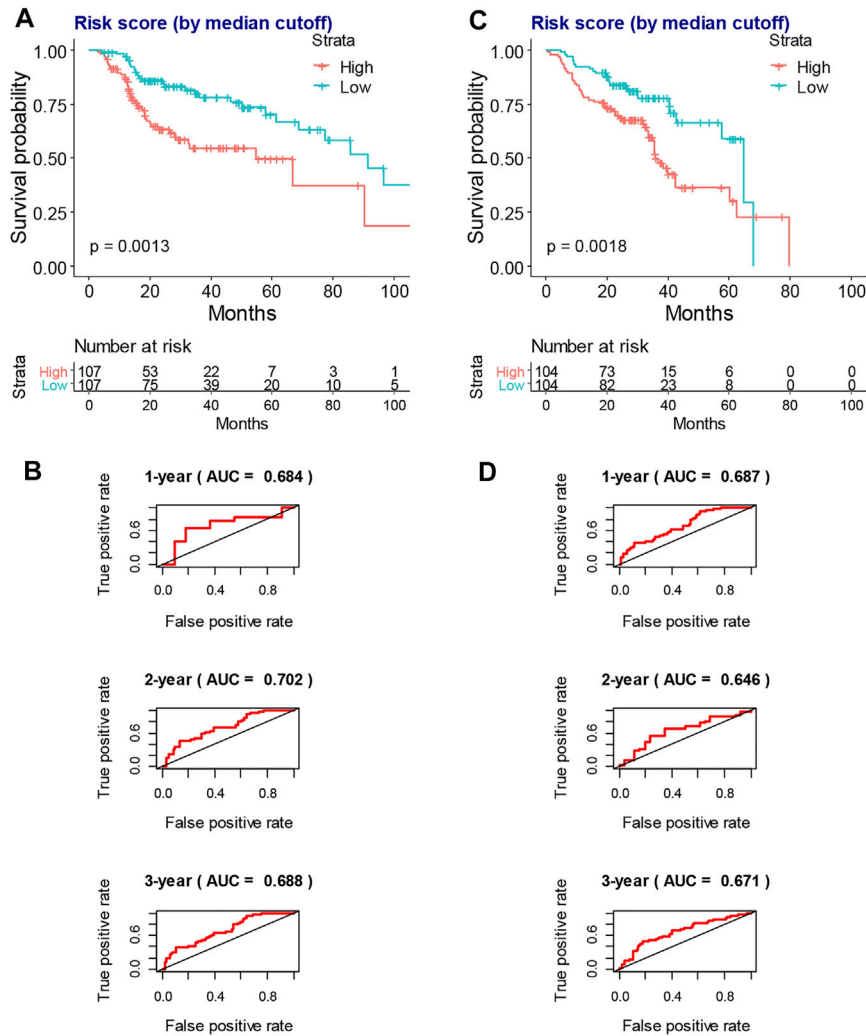


FIGURE 6 | The construction and validation of risk score model in the overall survival of locally advanced HNSCC patients. **(A)** The KM plot shows that higher risk score indicates worse overall survival of locally advanced TCGA-HNSCC patients who had RT. **(B)** The AUC plots of risk score to predict the 1-, 2-, and 3-year overall survival of locally advanced TCGA-HNSCC patients who had RT. **(C)** The KM plot shows that higher risk score indicates worse overall survival of locally advanced GSE65858-HNSCC patients. **(D)** The AUC plots of risk score to predict the 1-, 2-, and 3-year overall survival of locally advanced GSE65858-HNSCC patients. HNSCC, head and neck squamous cell carcinoma; KM, Kaplan–Meier; TCGA, The Cancer Genome Atlas; RT, radiotherapy; AUC, area under the receiver operating characteristic curve.

HDAC inhibitors could enhance the expression of cancer antigens, decrease immunosuppressive cell populations such as the myeloid-derived suppressor cells, and induce specific chemokine expression on T cells (Banik et al., 2019). HDAC inhibition was found to potentiate antitumor activity of macrophages and enhance anti-PD-L1-mediated tumor suppression (Li et al., 2021). Our study showed that trichostatin A had the potential to reverse the RR and immune suppression status of HNSCC and might thereby improve the prognosis of HNSCC, providing new bioinformatics evidences on the relationship between HDAC inhibitors and HNSCC. The combination of HDAC inhibitor with immunotherapy and RT might improve the therapeutic efficacy of HNSCC.

Our study had some limitations. First, TCGA is a retrospective database, which has a lower level of evidence. Second, the clinical

information from TCGA-HNSCC was often missed due to parameters such as surgery and chemotherapy application, the detailed information of RT, loco-regional control or response to RT, and HPV status. Our heterogeneous cohort in terms of grade or other clinical information might contribute to the different prognoses. Therefore, a prospective study of a homogenous HNSCC cohort is required to validate our study. Third, the GSE65858 from the GEO database had no information of RT experience, so we included all the locally advanced HNSCC samples for the survival analysis. We expect our results to be externally validated by a future study regarding RT and HNSCC. Fourth, the underlying mechanisms of HNSCC and the hub survival-related genes or trichostatin A should be further explored and characterized.

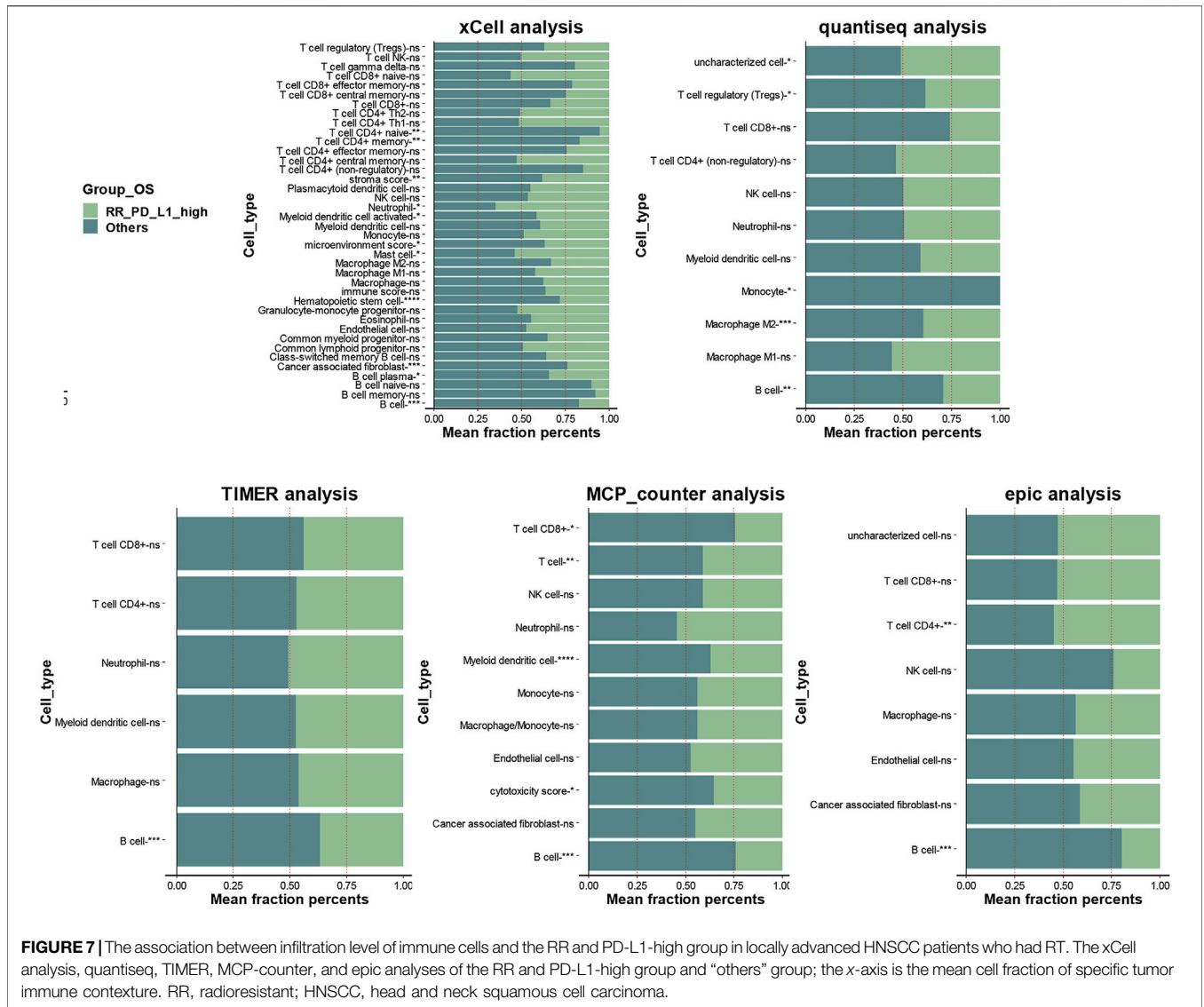


TABLE 3 | Key drugs that had potential therapeutic effects on RR and PD-L1-high group.

Drug	p-Value	FDR
Trichostatin A_MCF7	4.55E-17	1.63E-13
Trichostatin A_HL60	1.50E-06	2.68E-03
Trichostatin A_PC3	6.06E-06	7.25E-03

Note. RR, radioresistant; FDR, false discovery rate.

CONCLUSION

Our study found that a combination of 31-radiosensitivity gene signature and the expression level of PD-L1 had the potential

prognostic value for patients with locally advanced HNSCC who had RT. The RR and PD-L1-high group was significantly associated with worse clinical survival than other patients. The B cells were lower in the RR and PD-L1-high group. The identified risk gene signature of patients with locally advanced HNSCC and the potential therapeutic drug trichostatin A for the RR and PD-L1-high group are worth to be further investigated. Prospective studies are required to validate our findings in a homogenous, prospectively treated patient cohort.

DATA AVAILABILITY STATEMENT

The original contributions presented in the study are included in the article/**Supplementary Material**. Further inquiries can be directed to the corresponding author.

AUTHOR CONTRIBUTIONS

QW and DD designed the study. DD and YG analyzed the data. BJ and JL collected the data. The manuscript was written by DD, YG, and YS and then checked by QW. All authors reviewed and contributed to the manuscript.

FUNDING

This study was partially supported by the National Natural Science Foundation of China (Nos. 81572952, 82073332).

REFERENCES

- Aran, D., Hu, Z., and Butte, A. J. (2017). xCell: Digitally Portraying the Tissue Cellular Heterogeneity Landscape. *Genome Biol.* 18 (1), 220. doi:10.1186/s13059-017-1349-1
- Banik, D., Moufarrij, S., and Villagra, A. (2019). Immunoepigenetics Combination Therapies: An Overview of the Role of HDACs in Cancer Immunotherapy. *Int. J. Mol. Sci.* 20 (9). doi:10.3390/ijms20092241
- Becht, E., Giraldo, N. A., Lacroix, L., Buttard, B., Elarouci, N., Petitprez, F., et al. (2016). Estimating the Population Abundance of Tissue-Infiltrating Immune and Stromal Cell Populations Using Gene Expression. *Genome Biol.* 17 (1), 218. doi:10.1186/s13059-016-1070-5
- Bray, F., Ferlay, J., Soerjomataram, I., Siegel, R. L., Torre, L. A., and Jemal, A. (2018). Global Cancer Statistics 2018: GLOBOCAN Estimates of Incidence and Mortality Worldwide for 36 Cancers in 185 Countries. *CA Cancer J. Clin.* 68, 394–424. doi:10.3322/caac.21492
- Chajon, E., Castelli, J., Marsiglia, H., and De Crevoisier, R. (2017). The Synergistic Effect of Radiotherapy and Immunotherapy: A Promising but Not Simple Partnership. *Crit. Rev. Oncology/Hematology* 111, 124–132. doi:10.1016/j.critrevonc.2017.01.017
- Chan, J., Wang, X., Turner, J. A., Baldwin, N. E., and Gu, J. (2019). Breaking the Paradigm: Dr Insight Empowers Signature-free, Enhanced Drug Repurposing. *Bioinformatics* 35 (16), 2818–2826. doi:10.1093/bioinformatics/btz006
- Chen, J., Liu, A., Lin, Z., Wang, B., Chai, X., Chen, S., et al. (2020). Downregulation of the Circadian Rhythm Regulator HLF Promotes Multiple-Organ Distant Metastases in Non-small Cell Lung Cancer through PPAR/NF- κ B Signaling. *Cancer Lett.* 482, 56–71. doi:10.1016/j.canlet.2020.04.007
- Citro, S., Bellini, A., Miccolo, C., Ghiani, L., Carey, T. E., and Chiocca, S. (2019). Synergistic Antitumor Activity of HDAC Inhibitor SAHA and EGFR Inhibitor Gefitinib in Head and Neck Cancer: a Key Role for Δ Np63a. *Br. J. Cancer* 120 (6), 658–667. doi:10.1038/s41416-019-0394-9
- Finotello, F., Mayer, C., Plattner, C., Laschober, G., Rieder, D., Hackl, H., et al. (2019). Molecular and Pharmacological Modulators of the Tumor Immune Contexture Revealed by Deconvolution of RNA-Seq Data. *Genome Med.* 11 (1), 34. doi:10.1186/s13073-019-0638-6
- Franzè, E., Stolfi, C., Troncone, E., Scarozza, P., and Monteleone, G. (2020). Role of Interleukin-34 in Cancer. *Cancers (Basel)* 12 (1). doi:10.3390/cancers12010252
- Garber, S. T., Hashimoto, Y., Weathers, S.-P., Xiu, J., Gatalica, Z., Verhaak, R. G. W., et al. (2016). Immune Checkpoint Blockade as a Potential Therapeutic Target: Surveying CNS Malignancies. *Neuonc* 18 (10), 1357–1366. doi:10.1093/neuonc/now132
- García-Pedrero, J. M., Martínez-Cambor, P., Díaz-Coto, S., Munguía-Calzada, P., Vallina-Alvarez, A., Vázquez-Lopez, F., et al. (2017). Tumor Programmed Cell Death Ligand 1 Expression Correlates with Nodal Metastasis in Patients with Cutaneous Squamous Cell Carcinoma of the Head and Neck. *J. Am. Acad. Dermatol.* 77 (3), 527–533. doi:10.1016/j.jaad.2017.05.047
- Ghashghaei, M., Niazi, T. M., Aguilar-Mahecha, A., Klein, K. O., Greenwood, C. M. T., Basik, M., et al. (2019). Identification of a Radiosensitivity Molecular Signature Induced by Enzalutamide in Hormone-Sensitive and Hormone-Resistant Prostate Cancer Cells. *Sci. Rep.* 9 (1), 8838. doi:10.1038/s41598-019-44991-w

ACKNOWLEDGMENTS

The authors would like to thank Erzhen Wei, from Hangzhou Foreign languages School, for participating in the acquirement of the TCGA data from Xena database and the statistical analysis of this study.

SUPPLEMENTARY MATERIAL

The Supplementary Material for this article can be found online at: <https://www.frontiersin.org/articles/10.3389/fmolb.2021.775562/full#supplementary-material>

- Ghebeh, H., Mohammed, S., Al-Omair, A., Qattant, A., Lehe, C., Al-Qudaihi, G., et al. (2006). The B7-H1 (PD-L1) T Lymphocyte-Inhibitory Molecule Is Expressed in Breast Cancer Patients with Infiltrating Ductal Carcinoma: Correlation with Important High-Risk Prognostic Factors. *Neoplasia* 8 (3), 190–198. doi:10.1593/neo.05733
- Hanahan, D., and Weinberg, R. A. (2011). Hallmarks of Cancer: the Next Generation. *Cell* 144 (5), 646–674. doi:10.1016/j.cell.2011.02.013
- Hladíková, K., Koucký, V., Bouček, J., Laco, J., Grega, M., Hodek, M., et al. (2019). Tumor-infiltrating B Cells Affect the Progression of Oropharyngeal Squamous Cell Carcinoma via Cell-To-Cell Interactions with CD8+ T Cells. *J. Immunotherapy Cancer* 7 (1), 261. doi:10.1186/s40425-019-0726-6
- Huang, C.-Y., Huang, S.-P., Hsueh, Y.-M., Chen, L.-C., Lu, T.-L., and Bao, B.-Y. (2020). Genetic Analysis Identifies the Role of HLF in Renal Cell Carcinoma. *Cancer Genomics Proteomics* 17 (6), 827–833. doi:10.21873/cgp.20236
- Jang, B.-S., and Kim, I. A. (2018). A Radiosensitivity Gene Signature and PD-L1 Predict the Clinical Outcomes of Patients with Lower Grade Glioma in TCGA. *Radiother. Oncol.* 128 (2), 245–253. doi:10.1016/j.radonc.2018.05.003
- Jang, B.-S., and Kim, I. A. (2020). A Radiosensitivity Gene Signature and PD-L1 Status Predict Clinical Outcome of Patients with Glioblastoma Multiforme in the Cancer Genome Atlas Dataset. *Cancer Res. Treat.* 52 (2), 530–542. doi:10.4143/crt.2019.440
- Jang, B.-S., and Kim, I. A. (2017). A Radiosensitivity Gene Signature and PD-L1 Status Predict Clinical Outcome of Patients with Invasive Breast Carcinoma in the Cancer Genome Atlas (TCGA) Dataset. *Radiother. Oncol.* 124 (3), 403–410. doi:10.1016/j.radonc.2017.05.009
- Jia, L., Zhang, S., Huang, Y., Zheng, Y., and Gan, Y. (2017). Trichostatin A Increases Radiosensitization of Tongue Squamous Cell Carcinoma via miR-375. *Oncol. Rep.* 37 (1), 305–312. doi:10.3892/or.2016.5261
- Jung, S. N., Kang, Y. E., Lee, G. H., Liu, L., Oh, C., Jin, Y. L., et al. (2020). Brn3a/Pou4f1 Functions as a Tumor Suppressor by Targeting C-Met/stat3 Signaling in Thyroid Cancer. *J. Clin. Endocrinol. Metab.* 105 (9). doi:10.1210/clinem/dgaa316
- Kim, H. S., Kim, S. C., Kim, S. J., Park, C. H., Jeung, H.-C., Kim, Y. B., et al. (2012). Identification of a Radiosensitivity Signature Using Integrative Metaanalysis of Published Microarray Data for NCI-60 Cancer Cells. *BMC Genomics* 13, 348. doi:10.1186/1471-2164-13-348
- Kim, J., Hong, S. J., Park, J. H., Park, S. Y., Kim, S. W., Cho, E. Y., et al. (2009). Expression of Cystathionine Beta-Synthase Is Downregulated in Hepatocellular Carcinoma and Associated with Poor Prognosis. *Oncol. Rep.* 21 (6), 1449–1454. doi:10.3892/or.00000373
- Kim, S. S., Shen, S., Miyauchi, S., Sanders, P. D., Franiak-Pietryga, I., Mell, L., et al. (2020). B Cells Improve Overall Survival in HPV-Associated Squamous Cell Carcinomas and Are Activated by Radiation and PD-1 Blockade. *Clin. Cancer Res.* 26 (13), 3345–3359. doi:10.1158/1078-0432.ccr-19-3211
- Kulka, L. A. M., Fangmann, P.-V., Panfilova, D., and Olzscha, H. (2020). Impact of HDAC Inhibitors on Protein Quality Control Systems: Consequences for Precision Medicine in Malignant Disease. *Front. Cell Dev. Biol.* 8, 425. doi:10.3389/fcell.2020.00425
- Kumar, B., Yadav, A., Lang, J. C., Teknos, T. N., and Kumar, P. (2015). Suberoylanilide Hydroxamic Acid (SAHA) Reverses Chemoresistance in Head and Neck Cancer Cells by Targeting Cancer Stem Cells via the Downregulation of Nanog. *Genes Cancer* 6 (3–4), 169–181. doi:10.18632/genesandcancer.54

- Lamb, J. (2007). The Connectivity Map: a New Tool for Biomedical Research. *Nat. Rev. Cancer* 7 (1), 54–60. doi:10.1038/nrc2044
- Li, D., Yang, Z., Liu, Z., Zou, Q., and Yuan, Y. (2020). Clinical Significance of CBS and CCL21 in Gallbladder Adenocarcinomas and Squamous Cell/Adenosquamous Carcinomas. *Appl. Immunohistochem. Mol. Morphol.* 28 (2), 103–110. doi:10.1097/pai.0000000000000705
- Li, T., Fu, J., Zeng, Z., Cohen, D., Li, J., Chen, Q., et al. (2020). TIMER2.0 for Analysis of Tumor-Infiltrating Immune Cells. *Nucleic Acids Res.* 48 (W1), W509–W514. doi:10.1093/nar/gkaa407
- Li, X., Su, X., Liu, R., Pan, Y., Fang, J., Cao, L., et al. (2021). HDAC Inhibition Potentiates Anti-tumor Activity of Macrophages and Enhances Anti-PD-L1-mediated Tumor Suppression. *Oncogene* 40 (10), 1836–1850. doi:10.1038/s41388-020-01636-x
- Li, Y., and Seto, E. (2016). HDACs and HDAC Inhibitors in Cancer Development and Therapy. *Cold Spring Harb Perspect. Med.* 6 (10). doi:10.1101/cshperspect.a026831
- Lin, Y.-M., Sung, W.-W., Hsieh, M.-J., Tsai, S.-C., Lai, H.-W., Yang, S.-M., et al. (2015). High PD-L1 Expression Correlates with Metastasis and Poor Prognosis in Oral Squamous Cell Carcinoma. *PLoS One* 10 (11), e0142656. doi:10.1371/journal.pone.0142656
- Liu, B., Su, Q., Ma, J., Chen, C., Wang, L., Che, F., et al. (2021). Prognostic Value of Eight-Gene Signature in Head and Neck Squamous Carcinoma. *Front. Oncol.* 11, 657002. doi:10.3389/fonc.2021.657002
- Liu, C., Mann, D., Sinha, U. K., and Kokot, N. C. (2018). The Molecular Mechanisms of Increased Radiosensitivity of HPV-Positive Oropharyngeal Squamous Cell Carcinoma (OPSCC): an Extensive Review. *J. Otolaryngol. - Head Neck Surg.* 47 (1), 59. doi:10.1186/s40463-018-0302-y
- Liu, Y., Dong, Y., Kong, L., Shi, F., Zhu, H., and Yu, J. (2018). Abscopal Effect of Radiotherapy Combined with Immune Checkpoint Inhibitors. *J. Hematol. Oncol.* 11 (1), 104. doi:10.1186/s13045-018-0647-8
- Lyu, X., Zhang, M., Li, G., Jiang, Y., and Qiao, Q. (2019). PD-1 and PD-L1 Expression Predicts Radiosensitivity and Clinical Outcomes in Head and Neck Cancer and Is Associated with HPV Infection. *J. Cancer* 10 (4), 937–948. doi:10.7150/jca.27199
- Mary Goldman, B. C., Hastie, M., Repečka, K., Kamath, A., McDade, F., Rogers, D., et al. (2019). *The UCSC Xena Platform for Public and Private Cancer Genomics Data Visualization and Interpretation.* bioRxiv, 326470.
- McCarthy, D. J., Chen, Y., and Smyth, G. K. (2012). Differential Expression Analysis of Multifactor RNA-Seq Experiments with Respect to Biological Variation. *Nucleic Acids Res.* 40 (10), 4288–4297. doi:10.1093/nar/gks042
- Müller, T., Braun, M., Dietrich, D., Aktekin, S., Höft, S., Kristiansen, G., et al. (2017). PD-L1: a Novel Prognostic Biomarker in Head and Neck Squamous Cell Carcinoma. *Oncotarget* 8 (32), 52889–52900. doi:10.18632/oncotarget.17547
- Musa, A., Ghorai, L. S., Zhang, S. D., Glazko, G., Yli-Harja, O., Dehmer, M., et al. (2018). A Review of Connectivity Map and Computational Approaches in Pharmacogenomics. *Brief Bioinform* 19 (3), 506–523. doi:10.1093/bib/bbw112
- Ndisang, D., Lorenzato, F., Sindos, M., Khan, A., Singer, A., and Latchman, D. S. (2009). The HPV Cellular Transactivator Brn-3a Can Be Used to Predict Cervical Adenocarcinoma and Squamous Carcinoma Precancer Lesions in the Developed and Developing Worlds. *Obstet. Gynecol. Int.* 2009, 359457. doi:10.1155/2009/359457
- Pennock, G. K., and Chow, L. Q. M. (2015). The Evolving Role of Immune Checkpoint Inhibitors in Cancer Treatment. *The Oncologist* 20 (7), 812–822. doi:10.1634/theoncologist.2014-0422
- Racle, J., de Jonge, K., Baumgaertner, P., Speiser, D. E., and Gfeller, D. (2017). Simultaneous Enumeration of Cancer and Immune Cell Types from Bulk Tumor Gene Expression Data. *Elife* 6. doi:10.7554/eLife.26476
- Ran, X., and Yang, K. (2017). Inhibitors of the PD-1/pd-L1 axis for the Treatment of Head and Neck Cancer: Current Status and Future Perspectives. *Dddt* 11, 2007–2014. doi:10.2147/dddt.s140687
- Ritchie, M. E., Phipson, B., Wu, D., Hu, Y., Law, C. W., Shi, W., et al. (2015). Limma powers Differential Expression Analyses for RNA-Sequencing and Microarray Studies. *Nucleic Acids Res.* 43 (7), e47. doi:10.1093/nar/gkv007
- Sato, H., Okonogi, N., and Nakano, T. (2020). Rationale of Combination of Anti-PD-1/pd-L1 Antibody Therapy and Radiotherapy for Cancer Treatment. *Int. J. Clin. Oncol.* 25 (5), 801–809. doi:10.1007/s10147-020-01666-1
- Shirbhathe, E., Patel, P., Patel, V. K., Veerasamy, R., Sharma, P. C., and Rajak, H. (2020). The Combination of Histone Deacetylase Inhibitors and Radiotherapy: a Promising Novel Approach for Cancer Treatment. *Future Oncol.* 16 (30), 2457–2469. doi:10.2217/fon-2020-0385
- Strom, T., Harrison, L. B., Giuliano, A. R., Schell, M. J., Eschrich, S. A., Berglund, A., et al. (2017). Tumour Radiosensitivity Is Associated with Immune Activation in Solid Tumours. *Eur. J. Cancer* 84, 304–314. doi:10.1016/j.ejca.2017.08.001
- Subramanian, A., Narayan, R., Corsello, S. M., Peck, D. D., Natoli, T. E., Lu, X., et al. (2017). A Next Generation Connectivity Map: L1000 Platform and the First 1,000,000 Profiles. *Cell* 171 (6), 1437–1452. e1417. doi:10.1016/j.cell.2017.10.049
- Tang, L., Wei, F., Wu, Y., He, Y., Shi, L., Xiong, F., et al. (2018). Role of Metabolism in Cancer Cell Radioresistance and Radiosensitization Methods. *J. Exp. Clin. Cancer Res.* 37 (1), 87. doi:10.1186/s13046-018-0758-7
- Thompson, R. H., Gillett, M. D., Chevillet, J. C., Lohse, C. M., Dong, H., Webster, W. S., et al. (2004). Costimulatory B7-H1 in Renal Cell Carcinoma Patients: Indicator of Tumor Aggressiveness and Potential Therapeutic Target. *Proc. Natl. Acad. Sci.* 101 (49), 17174–17179. doi:10.1073/pnas.0406351101
- Topalian, S. L., Hodi, F. S., Brahmer, J. R., Gettinger, S. N., Smith, D. C., McDermott, D. F., et al. (2012). Safety, Activity, and Immune Correlates of Anti-PD-1 Antibody in Cancer. *N. Engl. J. Med.* 366 (26), 2443–2454. doi:10.1056/nejmoa1200690
- Vokes, E. E., Weichselbaum, R. R., Lippman, S. M., and Hong, W. K. (1993). Head and Neck Cancer. *N. Engl. J. Med.* 328 (3), 184–194. doi:10.1056/nejm199301213280306
- Wang, Y., Deng, W., Li, N., Neri, S., Sharma, A., Jiang, W., et al. (2018). Combining Immunotherapy and Radiotherapy for Cancer Treatment: Current Challenges and Future Directions. *Front. Pharmacol.* 9, 185. doi:10.3389/fphar.2018.00185
- Wang, Z., Zhu, J., Wang, T., Zhou, H., Wang, J., Huang, Z., et al. (2021). Loss of IL-34 Expression Indicates Poor Prognosis in Patients with Lung Adenocarcinoma. *Front. Oncol.* 11, 639724. doi:10.3389/fonc.2021.639724
- Wood, O., Woo, J., Seumois, G., Savelyeva, N., McCann, K. J., Singh, D., et al. (2016). Gene Expression Analysis of TIL Rich HPV-Driven Head and Neck Tumors Reveals a Distinct B-Cell Signature when Compared to HPV Independent Tumors. *Oncotarget* 7 (35), 56781–56797. doi:10.18632/oncotarget.10788
- Wouters, M. C. A., and Nelson, B. H. (2018). Prognostic Significance of Tumor-Infiltrating B Cells and Plasma Cells in Human Cancer. *Clin. Cancer Res.* 24 (24), 6125–6135. doi:10.1158/1078-0432.ccr-18-1481
- Xiang, X., Yu, P.-C., Long, D., Liao, X.-L., Zhang, S., You, X.-M., et al. (2018). Prognostic Value of PD -L1 Expression in Patients with Primary Solid Tumors. *Oncotarget* 9 (4), 5058–5072. doi:10.18632/oncotarget.23580
- You, G.-R., Cheng, A.-J., Lee, L.-Y., Huang, Y.-C., Liu, H., Chen, Y.-J., et al. (2019). Prognostic Signature Associated with Radioresistance in Head and Neck Cancer via Transcriptomic and Bioinformatic Analyses. *BMC Cancer* 19 (1), 64. doi:10.1186/s12885-018-5243-3

Conflict of Interest: The authors declare that the research was conducted in the absence of any commercial or financial relationships that could be construed as a potential conflict of interest.

Publisher's Note: All claims expressed in this article are solely those of the authors and do not necessarily represent those of their affiliated organizations, or those of the publisher, the editors, and the reviewers. Any product that may be evaluated in this article, or claim that may be made by its manufacturer, is not guaranteed or endorsed by the publisher.

Copyright © 2021 Dai, Guo, Shui, Li, Jiang and Wei. This is an open-access article distributed under the terms of the Creative Commons Attribution License (CC BY). The use, distribution or reproduction in other forums is permitted, provided the original author(s) and the copyright owner(s) are credited and that the original publication in this journal is cited, in accordance with accepted academic practice. No use, distribution or reproduction is permitted which does not comply with these terms.